



# CHALMERS

---

## **Electrochemical hydride formation in thin Pd films analyzed with a combined optical and electrochemical technique**

Master's thesis in Applied Physics

MATTIAS FREDRIKSSON

MASTER'S THESIS

# Electrochemical hydride formation in thin Pd films analyzed with a combined optical and electrochemical technique

Mattias Fredriksson

©Mattias Fredriksson, 2014

**Supervisor:** Björn Wickman, Chalmers

**Examiner:** Christoph Langhammer, Chalmers

Department of Applied Physics  
Division of Chemical Physics  
CHALMERS UNIVERSITY OF TECHNOLOGY  
SE-412 96 Gothenburg  
Sweden  
Telephone: +46 (0)31-772 1000

Gothenburg, Sweden 2014

## Abstract

The main objective of this work was to investigate how UV/Vis spectroscopy and electrochemical techniques can be combined to gain more information about the hydride formation in palladium thin-films. By controlling the potential in the electrochemical circuit, it is possible to control the hydride formation and by measuring the current, the amount of hydride formed can be quantified. Optical measurements were done in transmission and reflection mode and the response was synchronized with the electrochemical data.

Focus has been on hydride formation in palladium films of thickness 20 and 100 nm. The 100 nm films have been measured with reflection measurements, as light cannot pass through these thicknesses. For the 20 nm film, both reflection and transmission measurements have been carried out. The samples were placed in a flow cell that can measure both electrochemistry and UV/Vis response at the same time. The flow cell was filled with sulfuric acid electrolyte, and the potential was scanned between hydride and oxide formation regimes.

The result proves that hydride formation in palladium can be analyzed with a rather simple optical measurement with resolution corresponding to fractions of a monolayer, both for thicker and thinner films. The amount of hydride formed could be determined, even though the hydrogen evolution reaction interfered with the interpretation of the formed hydride. Hydrogen evolution reaction occurs below 0 V (vs. RHE) and caused problems for the flow cell as bubbles formed on both the working and counter electrode.

Preliminary measurements were also performed on platinum thin-films with a thickness of 0.5 and 1.5 nm. This showed promising results but more tests should be performed so that good conclusions can be made.

The main conclusion is that combining electrochemistry and optical techniques is a powerful tool that can give more understanding of the reactions taking place in, and on, materials used in fuel cell and hydrogen storage research. Optimizing the setup can lead to great new discoveries, driving the hydrogen economy even closer to realization.

## Acknowledgements

I would like to thank my examiner and supervisor Christoph Langhammer and Björn Wickman for giving me the opportunity to work in the interesting field of combining electrochemistry and optical measurements. A special thanks to my supervisor Björn Wickman who has been a great help and support throughout the work and who has pushed me to do things I otherwise try to avoid. I would like to thank my examiner Christoph Langhammer for discussing and helping me understand some of the optical phenomenon in the thin films. Carl Wadell also deserves to be mentioned as he helped me with understanding the Matlab code and also helped me when the optical measurements was behaving strangely.

Mattias Fredriksson, Göteborg July 18, 2014





# Contents

<b>1</b>	<b>Introduction</b>	<b>1</b>
<b>2</b>	<b>Background and Theory</b>	<b>3</b>
2.1	Electrochemistry . . . . .	3
2.1.1	3-Electrode-Setup . . . . .	3
2.1.2	Reference Electrode . . . . .	3
2.2	Optics . . . . .	5
2.2.1	Transmission . . . . .	5
2.2.2	Reflection . . . . .	6
2.3	Hydride formation in Palladium . . . . .	6
2.3.1	Hydrogen evolution reaction . . . . .	6
<b>3</b>	<b>Method and Experimental Setup</b>	<b>8</b>
3.1	Experimental and setup . . . . .	8
3.1.1	Flow Cell . . . . .	8
3.1.2	Experimental Setup . . . . .	8
3.1.3	Sample preparations . . . . .	10
3.2	Sample fabrication . . . . .	12
3.2.1	Pd sample fabrication . . . . .	12
3.2.2	Pt sample fabrication . . . . .	12
<b>4</b>	<b>Results and Discussion</b>	<b>13</b>
4.1	Pd thin film measurements . . . . .	13
4.1.1	Cyclic voltammetry . . . . .	13
4.1.2	H <sub>2</sub> evolution . . . . .	15
4.1.3	Origin of the optical response . . . . .	16
4.1.4	Thick Pd films . . . . .	18
4.1.5	SEM Analysis . . . . .	20

## CONTENTS

---

4.2	Pt thin film measurements . . . . .	22
4.2.1	1.5 nm Pt . . . . .	22
4.2.2	0.5 nm Pt . . . . .	22
<b>5</b>	<b>Conclusion</b>	<b>24</b>
<b>6</b>	<b>Outlook</b>	<b>25</b>
6.1	Pd outlook . . . . .	25
6.2	Setup Improvements . . . . .	25
6.2.1	Oxygen formation in the cell . . . . .	25
6.2.2	Uncompensated Resistance, $R_u$ . . . . .	26
6.2.3	Drift in optical signal . . . . .	26
	<b>Bibliography</b>	<b>28</b>
<b>A</b>	<b><math>R_u</math>-measurements</b>	<b>29</b>

# 1

## Introduction

TODAY'S SOCIETY IS heavily based upon the usage of fossil fuels, such as oil, gas, and coal. The human community must reach out and look for new sustainable ways of using resources so that this earth can sustain future generations. Several methods of producing and transporting energy have already been proposed, but none has the versatility that fossil fuel has in terms of storage, energy density, and simplicity to use. Batteries in cars are heavy and take time to charge and in the end, the energy in batteries must also come from somewhere, often from fossil fuels or nuclear power. Fuels from farmed crops, e.g. methanol, ethanol, and other kinds of biofuel will always compete with food production and/or wildlife. With the scarcity of food in large parts of the world this is not a sustainable option. A third alternative is hydrogen-based fuels, either in a combustion engine or in a fuel cell. Its non-poisonous nature makes it a good choice compared to fossil fuels from an emission and environmental perspective. The drawback with hydrogen ( $H_2$ ) fuels is that it takes a lot of energy to produce, and there is a need for better  $H_2$  storage.

There is also a need to find better materials for fuel cells and  $H_2$  storage. For  $H_2$  storage, palladium (Pd) is a good model system that has a high H/M ratio (M=metal), but it is both expensive due to its scarcity and has a high density, so it is not a viable option for consumer products. To find and analyze new materials there is also a need to find better measurement techniques so that it is possible to gain more knowledge. One way is to invent new systems that can extract more data, or one could combine two (or more) already existing methods so that different techniques complement each other. There are many techniques available today when one wants to combine different setups, but they are often expensive. To find a setup combination that is simple, cheap, and could extract a lot of data would be a great improvement. A recent study made by Johan Hagberg [1]

---

shows how standard electrochemistry and UV/Vis spectroscopy can be combined to create a simple but powerful tool for analyzing nanometer thin samples. Both of these tools are relatively cheap and do not take up too much space.

This thesis is about the continual testing of this new setup where electrochemistry and UV/Vis measurements have been done to see if it is possible to apply these combined techniques to learn more about the hydride formation in Pd. Electrochemistry has been the foundation with the combination of optical transmission and reflection measurements. Both systems have their own weakness, electrochemistry can only measure currents, and optics can only measure the extinction/reflection at a time interval. By synchronizing the optical data with the electrochemical data good precision can be acquired for the optical measurement. There are differences when comparing articles results regarding the maximum hydride formation for a Pd thin film. Ranges from 0.62 to 0.67 is common [2] but ratios as high as 0.73 has been reported [3], and it would be good if there was a way of knowing which result that is more probable. Preliminary measurements have also been done on Platinum (Pt) films to see how thin samples that can be probed.

# 2

## Background and Theory

### 2.1 Electrochemistry

Electrochemistry is a part of chemistry that involves charge transfer between a solid material electrode (a metal or semiconductor), and molecules on the surface. An ionic conductor, the electrolyte, is needed to transfer the charge between the cathode and the anode. The electrolyte used throughout this work has been sulfuric acid ( $\text{H}_2\text{SO}_4$ ). A common way of doing electrochemical measurements is by using a so called 3-electrode setup.

#### 2.1.1 3-Electrode-Setup

A schematic illustration of a 3-electrode-setup can be seen in figure 2.1. It consists of 3 electrodes; a working electrode (WE), a counter electrode (CE) and a reference electrode (RE).

For a 2-electrode-setup there is only a WE and a CE and this design can only measure the potential difference between the electrodes. By introducing a third electrode, a RE, there is now possible to measure an absolute potential for different systems. The 3-electrode-system is built so that a voltage is measured, or controlled, between the WE and the RE and the current flows between CE and WE.

#### 2.1.2 Reference Electrode

To be able to measure an absolute electrochemical potential of the charge build up in/on a metal one must have a well-defined system that can be measured against, and this system is called a RE.

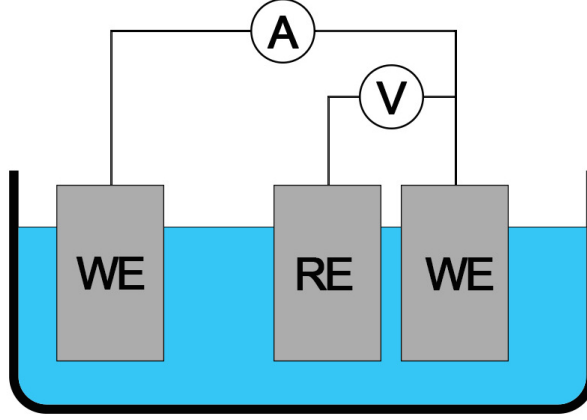


**Figure 2.1:** Schematic view of the 3-electrode setup

There is no absolute standard when it comes to measuring electrochemical potentials, but in this work Reversible Hydrogen Electrodes (RHE), a subtype of Standard Hydrogen Electrode (SHE), was of interest. SHE is defined as a Pt electrode that is submerged in hydrochloric acid and then bubbled with hydrogen ( $H_2$ ). The voltage should be zero at an activity of unity (which gives an concentration of HCl of 1.14 M) and a hydrogen pressure at one bar. [4] The RHE is defined similar to SHE but also take into account the pH-change in the electrolyte. The relation between SHE and RHE can be seen below:

$$E_{RHE} = E_{SHE} - 0.059 \times pH \quad (2.1)$$

In this work a mercury/mercury-sulfate ( $Hg/Hg_2SO_4$ ) electrode has been used, and the main reason for this is that the electrode is chlorine free. This is good as chlorine otherwise can poison the Pd surface. The other reason is that both the electrolyte and the RE have a similar chemical composition. Both have the sulfate group ( $SO_4^{-2}$ ) attached to it, which means that there is a limited transport between the electrolyte and the electrode. The relation between the  $Hg/Hg_2SO_4$  electrode and RHE scale is:

$$E_{RHE} = E_{Hg/HgSO_4} + 0.68 - 0.059 \times pH \quad (2.2)$$

where the pH for 0.5 M of  $H_2SO_4$  is close to 0.3 [5]. All potentials are measured against the RHE scale in this work.

## 2.2 Optics

Optical measurements throughout this work have been transmission (later plotted as extinction) and reflection measurements. When a reaction takes place in the bulk or on the surface of the material, the refractive index and dielectric function will change. This will slightly change the spectra and therefor change the measured reflection and extinction.

### 2.2.1 Transmission

When a beam of light passes through a material it can lose intensity in two ways, either by scattering of the light by the sample, or by absorption in the sample. The light that does not get astray in the sample will pass trough with an intensity loss. For a transmission sample it is possible to estimate the amount of hydrogen that has been absorbed into the sample by Lambert-Beers law [6] which is derived from:

$$\frac{dI_x}{dx} = \alpha \times c \times I_x \quad (2.3)$$

where  $\alpha$  is the absorption coefficient,  $I_x$  the intensity in x direction, and c is the concentration.  $dI_x/dx$  is the intensity change with an infinitesimal step in x direction. By separating and integrating the equation, and knowing that the intensity of the incoming light at  $x=0$  is  $I_0$ , gives:

$$\ln(I) = \alpha \times x \times \ln(I_0) \quad (2.4)$$

Rearrangement of the equation then yields:

$$C_H = -\frac{1}{\alpha \times d} \times \ln\left(\frac{I_1}{I_0}\right) \quad (2.5)$$

where  $C_H$  is the hydrogen concentration [H/Pd], d is the film thickness,  $\alpha$  is the absorption coefficient and  $I/I_0$  is the relative transmittance.  $I_0$  is the incident light and I the transmitted light. The absorption coefficient is defined as:

$$\alpha = \frac{4\pi\epsilon_r}{\lambda} \quad (2.6)$$

where  $\lambda$  is the wave length,  $\epsilon_r$  is the dielectric function of a metal and is  $\epsilon_r(\omega) = 1 + \chi_e$  ( $\chi_e$  is the electric susceptibility). The transmission data has been plotted as extinction, which is described as a combination of scattering and absorption of light in a material. The extinction is defined as:

$$Ext = 1 - \frac{S_m}{S_{ref}} \quad (2.7)$$

where  $S_m$  is the measured spectra and  $S_{ref}$  is the self-reference.



### 2.2.2 Reflection

Reflection can be divided into two groups, diffuse and specular reflection. Diffuse reflection describes reflectivity for an opaque, non-clear material, whereas specular reflection comes from a polished surface. Reflection can be derived from the optical theorem:

$$E = A + S \quad (2.8)$$

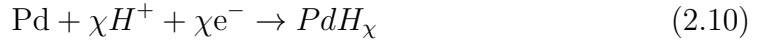
Where E is the extinction, A is the absorption, and S is scattering. S is a sum of the specular and diffuse reflection. In this work, only the specular reflection is taken into account as the surface where a metal Pd thin film. The reflection measurements is defined as:

$$RefI = \frac{S_m}{S_{ref}} - 1 \quad (2.9)$$

where  $S_m$  is the measured spectra and  $S_{ref}$  is the self-reference.

## 2.3 Hydride formation in Palladium

When Pd is exposed to a  $H_2$  pressure, either in gas or liquid phase, hydride formation starts to form in the Pd sample. For an electrochemical setup in acidic electrolyte, the hydride is formed via protons from the solution. The reaction for Palladium hydride (PdH) in an acidic solution is below:



Finding the H/Pd ratio was done by finding the charge by integrating the current. Assuming one  $e^-$  per absorbed/desorbed H the amount of hydride can be quantified using the electrode volume and the molar volume for Pd ( $8.56 \times 10^{-6} \text{ m}^3/\text{mol}$ ).

The maximum H/Pd ratio can be as high as 0.62-0.71, but to reach these values, thin samples with a thickness between a few monolayers to some  $\mu\text{m}$  are needed [7]. The reason for this is that a thick film does not get saturated under a cyclic voltammetry (CV) scan and therefore the high H/Pd ratios cannot be achieved. Not only does the thickness of the film has an important part in the absorption, but also the preparation of the film is of importance. There has been some contradiction when considering the microstructure generated by different sample preparation methods for the absorption. This will be discussed more in chapter 4.1.1.

### 2.3.1 Hydrogen evolution reaction

Below 0 V it is thermodynamically allowed to form  $H_2$  from protons via the hydrogen evolution reaction (HER). Pd has been shown to have a rather small barrier

(overpotential) for HER and, thus, it is likely that both hydrogen evolution and formation of PdH in the sample occurs at the same time when the potential is below 0 V. This makes it hard to separate the processes. A clear understanding of these processes is needed if one wants to find the exact H/Pd ratios for the Pd system, as both absorption and HER will contribute to the total current measured from the system. When HER occurs it is not possible to simply integrate the current to get the amount of hydrogen absorbed. If the HER could be measured with good accuracy it should be possible to subtract the HER current and from there isolate the current from the absorption alone. When determining the amount of hydride that is desorbing in the Pd film, it is of importance that the surrounding around the WE is free from dissolved  $H_2$  as this can give an overestimate of the desorbed hydride.

# 3

## Method and Experimental Setup

### 3.1 Experimental and setup

The setup consisted of a custom-made flow cell where both electrochemical and optical measurements could be performed at the same time. The electrochemical measurements were performed with a 3-electrode configuration where the WE was a Pd thin-film, the CE a Pt wire, and the RE was an Hg/Hg<sub>2</sub>SO<sub>4</sub> reference electrode. The electrodes were connected to a potentiostat and the transmitted or reflected light intensities through/from the film were measured by a spectrometer.

#### 3.1.1 Flow Cell

The flow cell used in this work was made out of Polyetheretherketone (PEEK), an organic polymer thermoplastic. A picture of the cell is shown in figure 3.1a, and the WE with the Cu tape is shown in figure 3.1b. The cell body was composed of three sections: i) a top part which clamps a window of quartz glass. ii) a middle part with a circular hole that constitutes the electrochemical cell volume and has a coiled Pt wire serving as CE, and channels for electrolyte inlet and outlet. iii) a bottom part which clamps the sample, which is connected as WE. Both the quartz window and sample are sealed with Viton<sup>®</sup> O-rings. On the WE, copper tape was attached to the area outside of the O-ring and connected to the potentiostat.

#### 3.1.2 Experimental Setup

The electrochemical measurements took place in a custom-made flow cell that from the inlet was connected through a Tygon<sup>®</sup> tube to a glass flask that contained the electrolyte (0.5 M sulfuric acid). The electrolyte was bubbled with an inert gas, in

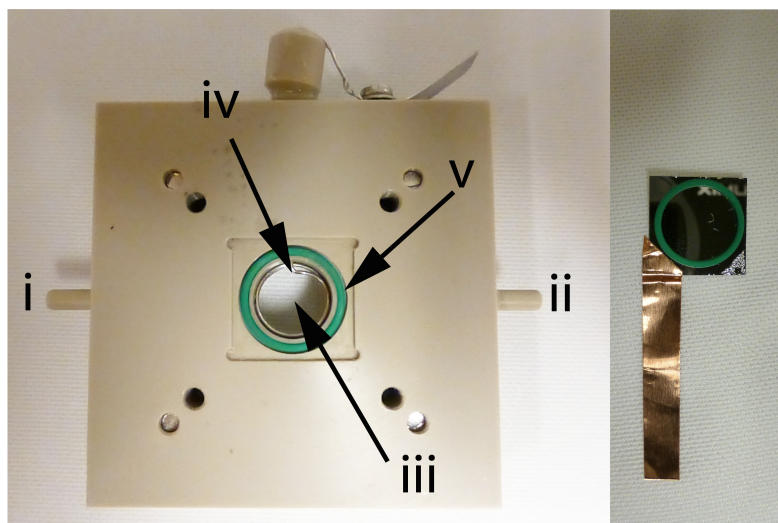


**Figure 3.1:** The flow cell used. i) Inlet, ii) outlet, iii) quartz window, iv) counter electrode, and v) O-ring. b) The working electrode with the Cu-tape attached.

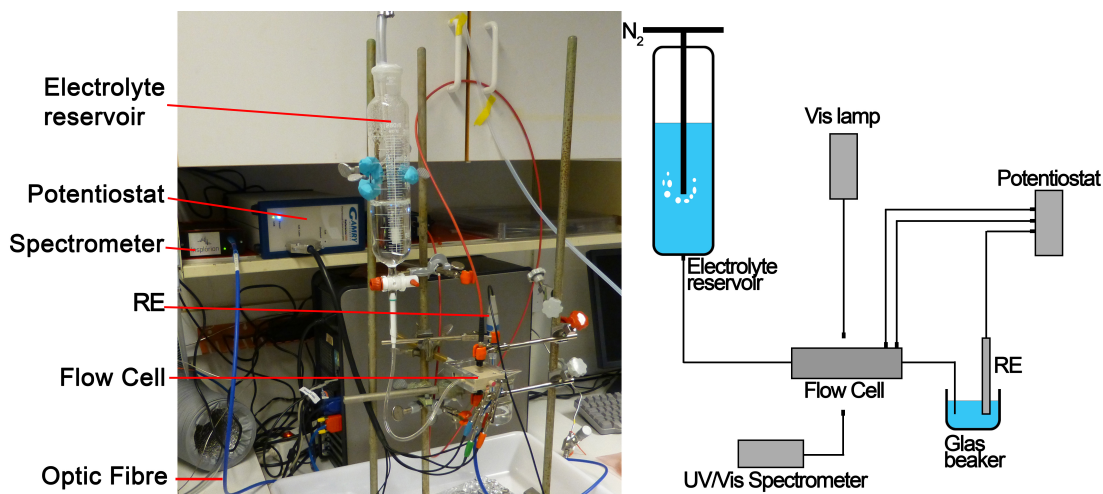


**Figure 3.2:** The setup used for all the electrochemical experiments (left), and a schematic image of the setup (right)

this case  $N_2$ , to exclude  $O_2$  from the system. The exit of the flow cell was connected to another glass beaker, also through a Tygon<sup>®</sup> tube, where a XR200 Radiometer Hg/Hg<sub>2</sub>SO<sub>4</sub> reference electrode was located. The Potentiostat, a Gamry Reference 600<sup>TM</sup> Potentiostat, was connected to the WE and CE inside the flow cell by two external connectors. A picture of the experimental setup can be seen in figure 3.2a, and a schematic view is seen in figure 3.2b.

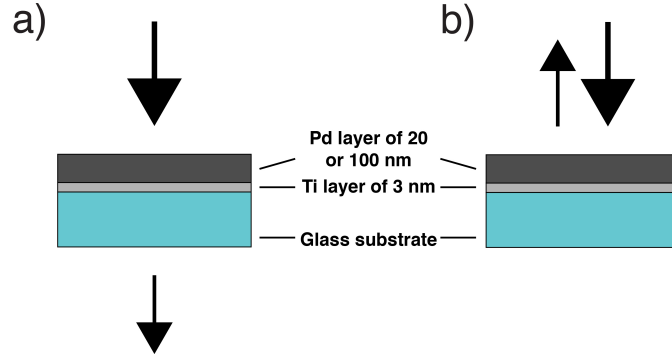


**Figure 3.3:** a) a schematic image of a transmission measurement. b) schematic image of a reflective measurement.

The optical measurements were performed by an Avantes Ava-Light HAL light source shining white light on the sample. The reflected or transmitted light was analyzed in an Avantes AvaSpec-HS1024x58TEC spectrometer. Depending on the type of measurement (transmission or reflection) small differences in the setup was used. For transmission experiments, figure 3.3a, an optical fiber fitted with a collimating lens from the light source shone light through the sample. The light that was not absorbed or scattered by the sample was collected by another cable fitted with a collimating lens at the other side of the sample. For the reflection, figure 3.3b, the light was sent from the lamp to the sample through a fiber bundle. The center fiber was used to collect the reflected light and the light from the outer fibers were used to probe the sample. Matlab<sup>®</sup> was used to collect the optical data.

### 3.1.3 Sample preparations

Before mounting the sample into the flow cell, a pre-cleaning procedure was performed. This cleaning procedure consists of 6 steps:

1. Submerge sample in a beaker with acetone, sonicate for 5 minutes.
2. Rinse with MilliQ-water.

3. Submerge sample in a beaker with isopropanol, sonicate for 5 minutes.
4. Rinse with MilliQ-water.
5. Submerge sample in a beaker with MilliQ-water, sonicate for 5 minutes.
6. Dry the sample with  $N_2$  flow.

After the sample was dried, a piece of copper tape was attached to one corner of the film, see figure 3.1b, and then mounted in the flow cell. The sample was then cleaned by CV through a series of steps:

1. 2 cycles, 20 mV/s, 0.32 V-0.66 V, iR-comp none.
2. Find representative  $R_u$ -value through simplified EIS-test.
3. 2 cycles, 5 mV/s, 2.3 mV-0.66 V, iR-comp  $0.85 \times R_u$ .
4. Wait for 3 minutes.
5. Repeat step 3 and 4 until the sample has reached a typical shape.

The first point is a pre-cleaning step with a fast scan rate of 20 mV/s between 0.32 V and 0.66 V. This step was there to confirm that there was no contact problem with the sample so that representative uncompensated resistance ( $R_u$ )-values could be acquired. The second step is a series of simplified electrochemical impedance spectroscopy (EIS) tests so that  $R_u$  was found. The representative values from the simplified EIS-test were then estimated by taking the mean of the data. iR-compensation were set to  $0.85 \times R_u$ . The third and fourth step was the cleaning-steps where the sample was cycled between the double layer region down to just before the onset of HER. After 2 cycles there was a small waiting period of 3 minutes before the process was started over from step 3. This continued until a fixed amount of cycles had been performed, or if the CV had reached a typical shape before the last cycles had been completed. This procedure gave different results than other people has got [7], see discussion on page 4.1.1, but it gave a large H/Pd ratio that was favourable for this work.

When cycling to the oxide formation region there will be a small corrosion to the Pd film surface. This is due to reorganization of the surface layer when oxide is forming, and when the oxide later desorb it will strip of some of the Pd atoms in the film. Extended cycling in the oxide region will corrode the sample to a state where the cycled film thickness is not the same as the uncycled one [8]. Because of this the oxide region was excluded when cleaning the sample though CV. The film does not corrode at lower potentials, in the hydride formation region, but due to HER and oxygen formation on the CE, negative potentials was omitted.

## 3.2 Sample fabrication

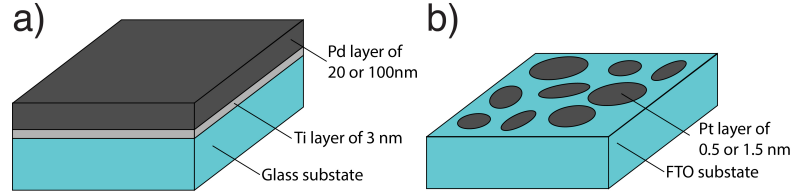


**Figure 3.4:** A schematic image of the Pd electrodes. b) A schematic image of the Pt electrodes.

### 3.2.1 Pd sample fabrication

The samples were fabricated by Björn Wickman in the MC2 cleanroom facility and the most important steps are described below; Samples of borofloat glass with a thickness of 0.5 mm were cut to 15×15 mm pieces and cleaned with the same method as described in section 3.1.2. After cleaning, the substrate was mounted into an E-beam evaporator (Lesker PVD 225 with a base pressure  $< 5 \times 10^{-7}$  mbar). A 3 nm thin titanium film was used as an adhesive layer before 20 or 100 nm of Pd was evaporated. The titanium adhesive layer has the effect of creating strong bonding between itself and the Pd film. Without the adhesive layer the Pd would detach from the glass as the stress in the film increases when the hydride is formed [9]. Figure 3.4a shows a schematic view of the Pd sample.

### 3.2.2 Pt sample fabrication

The Pt samples were also fabricated by Björn Wickman in the MC2 cleanroom facility using the same techniques as the Pd samples. But for those samples, Fluorine doped Tin Oxide (FTO) substrates with a thickness of 0.5 nm were used. After cleaning and mounting the sample in the E-beam evaporator a thin film of 0.5 or 1.5 nm Pt was evaporated directly onto the FTO. The amount of material evaporated was not enough to cover the whole substrate and therefore islands were formed, see figure 3.4b for a schematic view. The reason that an FTO substrate was used was because of the island formation. Without a conducting substrate there would be no contact between the different islands, and no measurements could be made.

# 4

## Results and Discussion

### 4.1 Pd thin film measurements

The main results from the measurements are shown below. All optical measurements have been carried out with white light. The data have been analyzed with a wavelength of 700 nm with an average of  $\pm 5$  nm to get a better signal to noise ratio.

#### 4.1.1 Cyclic voltammetry

The sample in figure 4.1 is a 20 nm thin Pd film that has been used in cyclic voltammetry with a scan rate of 5 mV/s. Figure 4.1a is the cyclic voltammogram, figure 4.1b the extinction and 4.1c shows the optical measurements, both for top and bottom.

Starting from 5 V and going cathodic (scanning toward lower potential) to the hydride formation, there is a peak showing up at around 0.17 V. This peak is mainly attributed to H<sub>2</sub> adsorption on the Pd surface [10]. H<sub>2</sub> absorption starts to be dominant at around 0.1 V due to the formation of  $\beta$  hydride inside the film. This formation rate reaches a maximum around 0.016 V where it then slows down. At -0.03 V the hydride formation rate has slowed down considerably but instead HER is occurring. At the turning point at -0.066 V, anodic, H<sub>2</sub> desorption starts to occur. The first peak at -0.034 V is attributed to the HER, as a bigger HER will give a bigger peak. Right after the first peak ends at 0.005 V the H<sub>2</sub> desorption peaks starts and reaches a maximum desorption rate at 0.05 V. Around 0.215 V there is a small peak attributed to the release of adsorbed H<sub>2</sub> on the surface. This peak together with the cathodic peak are in many cases right on top of each other



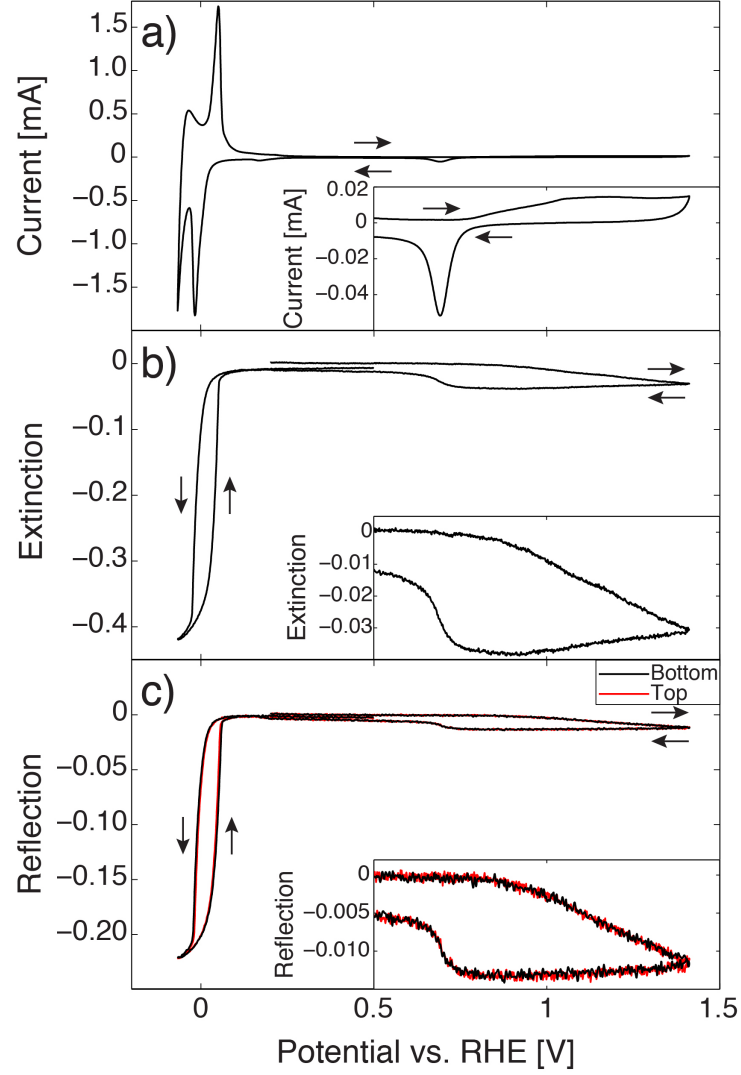


**Figure 4.1:** CV for a 20 nm Pd electrode scanned from oxide to hydride region, inset is focused to the oxide region. b) Extinction measurements for 20 nm Pd, inset is focus on the oxide region. c) Reflection measurement for top (red line) and bottom (black line), inset is focus on the oxide region.

[7] but in this case they have shifted apart. This shift might have something to do with the cleaning procedure that were performed to achieve a system with same starting point for all subsequent measurements. Anodic of 0.75 V,  $O_2$  starts to adsorb on the surface and reaches a maximum adsorption rate at 1.1 V. At 1.413 V there is a shift to cathodic cycling, but due to none reversibility of the  $O_2$  adsorption, it is not until around 0.8 V that  $O_2$  really starts to desorb.

Figure 4.1b and 4.1c shows the extinction and reflection measurement for a 20 nm Pd thin film. For the extinction measurements there is almost a doubling in the optical response compared to the reflection measurements (both at the hydride formation and oxide formation), other than that the two graphs are almost identical. For the reflection measurements in 4.1c the graphs are almost identical when comparing the top and the bottom measurement. The curves fit perfectly except for the hydride layer where the top measurement has a little narrower fit compared to the bottom measurement. This small difference will however give a big difference in the H/Pd ratio, which will be described in section 4.1.3.

The optical measurement, when compared to the CV, shows a good response to the forming of oxide and hydride. On the other hand, the optical measurements always have a small offset from the starting point to the endpoint in each cycle due to corrosion that happen on the oxide layer of the Pd film.

Horkans shows that an unannealed film has a higher absorption ratio than bulk Pd, and this might be attributed to the higher density of grains in the unannealed film. When the thin film is annealed, the grains will fuse together and the grain density will decrease. This annealing, he says, can decrease the ability to absorb  $H_2$  [11]. This theory is however not consistent with the results from the cleaning process in this work. Cleaning with CV (extended cycling can be comparable to an annealing process) makes the Pd film absorb more  $H_2$ , and at the same time there is a growth of the grains, as seen in figure 4.5.

### 4.1.2 $H_2$ evolution

When cycling to low potentials, below 0 V, HER might occur which make it hard to exclude the  $H_2$  in the vicinity of the electrode. Figure 4.2 shows how HER depends on the voltage for a 20 nm Pd film. Each point in figure 4.2 represents the average of 5 measurements, and the bars represents the standard deviation for these 5 measurements. It is clearly seen that before 0 V there was no current due to HER. It is not until around -0.01 V that HER starts being noticed. At 0.0277 V, represented by the blue dot and highlighted with a blue arrow, the current due to HER is  $10.62 \mu A$ , which corresponds to 1.58% of the current from HER and absorb. The current generated by HER is so small that it is fair to say that only absorption and desorption is attributed to the total current generated. At 0.0377V, red dot and highlighted with a red arrow, a current of  $22.29 \mu A$  is generated due to HER,

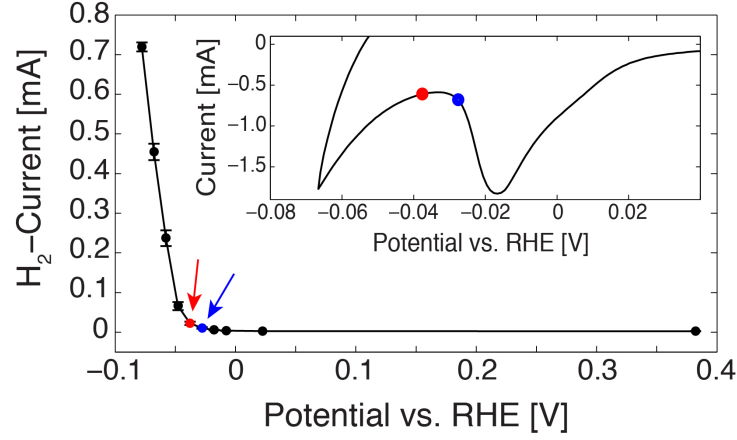


**Figure 4.2:** Hydrogen evolution for a 20 nm Pd film, inset is focused on the hydride region for the CV in figure 4.1a

which correspond to 3.64% of the total current. This starts to be a substantial part of the total current and therefore it is not feasible to continue integrate the current below this value to acquire the total amount of absorbed/desorbed  $H_2$ . Since the HER is exponentially growing it means that there will be a fast increase of  $H_2$  formation when going to lower potentials.

When looking at the same points in the CV, see inset of the figure 4.2, one can see that the first point (blue) is before the local maxima and the second point (red) is on the other side of this maxima. The existence of this type of local maxima is an indication that two processes are taking place at the same time. In this case, the most likely situation is that the first process, hydride formation is almost complete and thus the absolute current is decreasing and the second process,  $H_2$  evolution sets in, which creates a large negative current.

### 4.1.3 Origin of the optical response

When no other reactions than hydrogen absorption occur it is possible to calculate the hydride formation by integrating the current. This is true for potentials above 0 V, but below this value HER will give an extra contribution to the total current. It should be possible to subtract the current due to HER, but in this work the whole current is integrated. The blue and red dots from figure 4.2 has been converted to dashed lines in figure 4.3.

Figure 4.3a shows the potential as a function of the charge. Starting at the top of the black line and going downward it can be seen that for potentials of 0.4 V to around 0.2 V there is no hydride forming, as the potential is not enough to form hydride. After 0.2 V there is a small increase of hydride as  $\alpha$ -phase is forming.

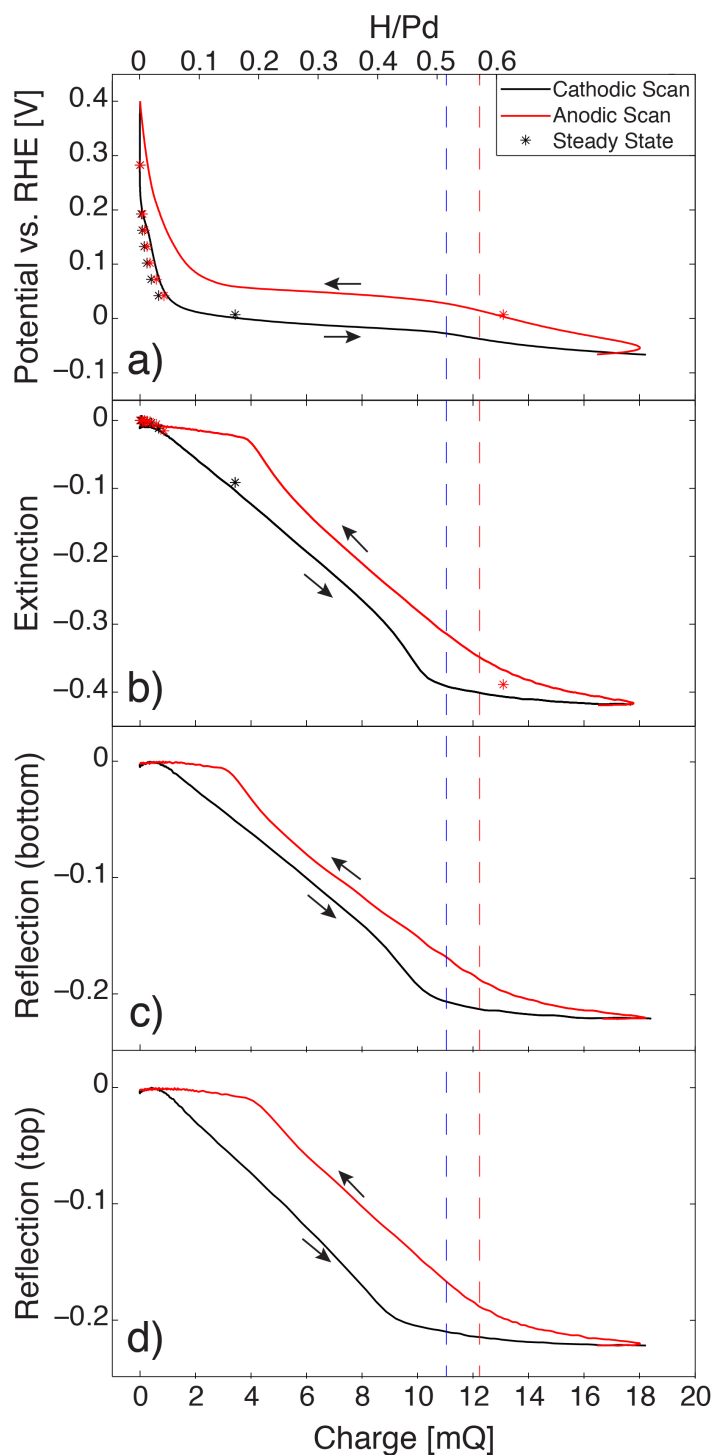


**Figure 4.3:** Charge vs. a) CV, b) Extinction, c) reflection(bottom), and d) reflection (top) for a 20nm Pd film. The top axis is scaled to H/Pd ratio and the blue and red line corresponds to the blue and red dot in figure 4.1 respectively. For a) and b) steady state points are plotted.

Right before the 0.0 V there is a huge change in charge due to the  $\beta$ -phase hydride that is forming. This trend holds until around 11 mQ when there is a break in the trend and the plot should turn downward, as the  $\beta$ -phase is saturated and no further hydride could be formed. Instead of this downward slope there is only a small increase of the slope as the charge continues to increase. This increase of the charge is due to the hydrogen evolution. On the way back, red line, the trend of the data has the same shape but with a slight hysteresis. In figure 4.3b, the transmission is plotted against the charge. From the black line at 0 mQ and going towards higher charge (cathodic scan), it is seen that there is no real change in extinction until around 0.25 mQ. After this the extinction rises linearly until it flattens out at around 11 mQ. At the red line on the way back (anodic scan) the same shape of the curve is seen, but with a hysteresis like figure 4.3a. Anodic at 4 mQ the charge flattens out at an extinction of 0. This means that even though there still is some charge (hydride) left in the film there is no optical response when the last hydride is desorbing. The reason for this is still unknown and should be tested further.

In figure 4.3a and 4.3b, static points at certain values were taken to see if the hysteresis would disappear completely or if it still would be some. For the figures it is seen that the hysteresis is almost completely gone. More points later on would be good to have but due to the HER at the lower potentials there was too much oxygen created at the CE to perform the measurements.

The same trends as for the transmission can also be seen for the reflection measurements (both top and bottom), figure 4.3cd, with the difference that the reflection measurement has half the optical response compared to the extinction measurement. This is the same size difference as for figure 4.1bc. The difference between figure 4.3c and 4.3d is the shape of the optical response curve. Reflection from the bottom, figure 4.3c, has a much smaller hysteresis than the reflection measurement, figure 4.3d. Why there is such a large hysteresis between the three different optical response curves is still unknown and therefore more test should be performed to learn why it turns out like this.

#### 4.1.4 Thick Pd films

Thicker Pd films were tested to see the difference in signal between a 100 nm and a 20 nm film. Figure 4.4a shows the CV for a 100 nm film and a 20 nm film. In the case with thicker films, extinction measurements cannot be used because the film is too thick. Instead a reflection measurement was used on both sides of the film to see if, and how, hydride formation could be seen. The reflection measurement can interact a small distance into the material which can be seen in thinner films. It is clearly evident that both top and bottom measurements can see the oxidation in figure 4.4c, as both plots are almost identical. However, the same cannot be done

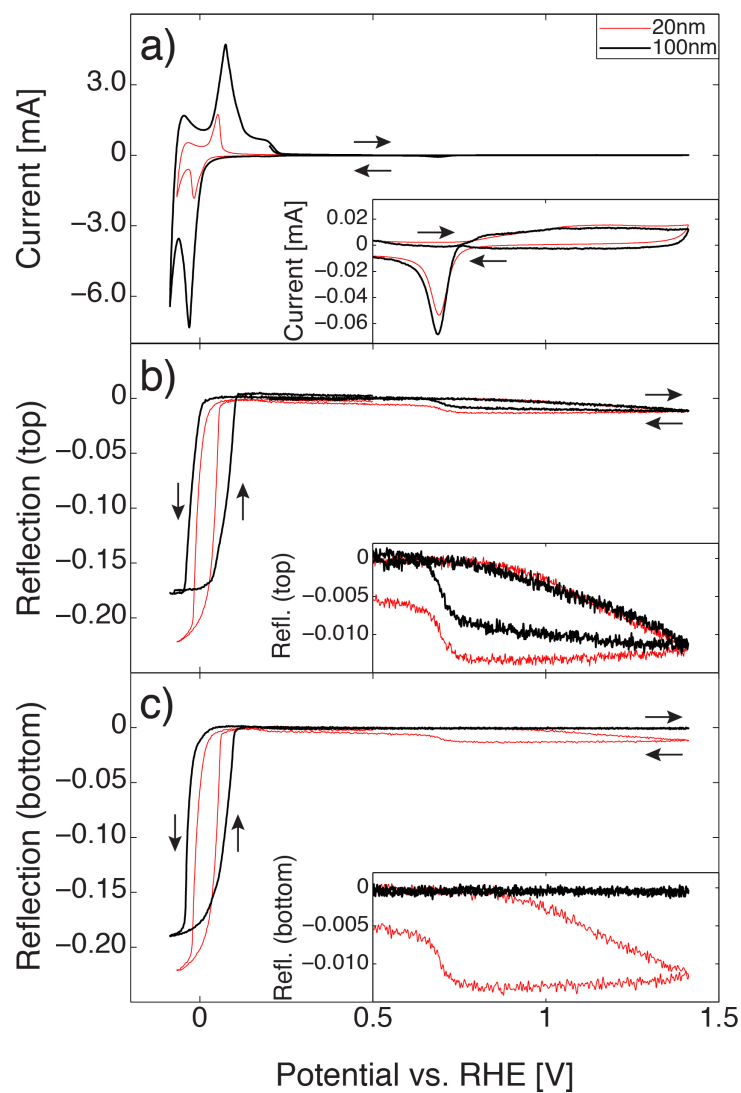


**Figure 4.4:** a) cyclic voltammogram for (red) 20 nm and (black) 100 nm Pd film. b) top reflection measurement for the (red) 20 nm and (black) 100 nm Pd film and c) bottom reflection measurement for the (red) 20 nm and (black) 100 nm Pd film

for a 100 nm film as the thickness of the film is too deep to penetrate. Somewhere in-between these film thicknesses there should be a maximum thickness that the reflection just barely can pass through.

The difference between the 100 nm and 20 nm film, figure 4.4a, is the higher current in the hydride region. This is no surprise since the 100 nm film has a greater volume than the 20 nm film and therefore can absorb more hydrogen, giving rise to larger currents. The current in the hydride absorption region for 100 and 20 nm is 7.33 A and 1.83 A respectively. The 100 nm film also has a wider hydride region (larger hysteresis) than the 20 nm samples. In the oxide region it is seen that the 100 nm film has a slightly larger hydrogen absorption/desorption peak than the 20 nm film. This might be because of the larger surface area, due to larger grain size of the 100 nm film. The shape of 100 nm sample has some strange shape cathodic around 0.76 V where the current turns upwards before the oxygen desorption.

Figure 4.4c is the bottom measurement of the reflection. The data in the oxide region shows what is expected for a thicker film compared to the top measurement. As the light cannot penetrate the sample the measured value is 0. This is compared to the bottom measurement of the 20 nm film, figure 4.1c, which shows an equal strong reflection as for the 20 nm top measurement.

A big issue with the flow cell when measuring Pd films is the formation of oxygen at the CE. When measuring Pd films, big currents are generated when the potential reaches the hydride formation zone. This gives rise to an equally big current on the CE which will start to create oxygen in the cell. If the sample, or the measurement currently used, is effected by oxygen this can have dire consequences for the end-results.

Tests were done to see if placement of the CE outside the flow cell (together with the RE) could be done to eliminate oxygen inside the cell. However, when placing the CE outside the cell there was a large change in the  $R_u$  measured (from  $\sim 10$  to  $4000 \Omega$ ) that excluded use of the CE outside the cell. If this could be solved both  $R_u$  and oxygen formation might be fixed with only one change. A more detailed explanation of this can be found in Appendix A.

#### 4.1.5 SEM Analysis

After some initial confusion about the change in the visual optical properties of the 100 nm films, a SEM analysis of the samples was performed to see if there were any big differences before and after cycling the samples. The images were taken by my supervisor after discussing which samples that needed to be included.

The evaporated film starts out with small grains, but thermodynamically it is more favourable to form larger grains. What is happening is that when cycling the film the grains will start to fuse together creating larger grains, similar to an

annealing process. If the film is thin, as for the 20 nm sample, there is not enough material to form the large grains that are seen for the 100 nm sample. This fusion of grains into larger ones might be the reason that the CV changes dramatically after several cycles.

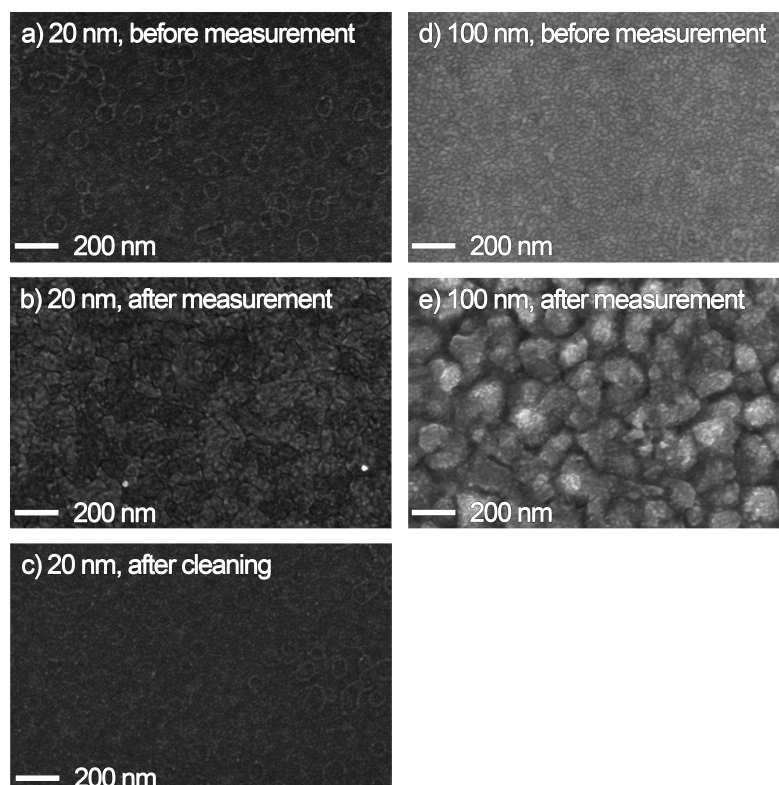


**Figure 4.5:** a) 20 nm after cleaning, before measurement. b) 20 nm after measurement. c) 20 nm after cleaning. Figure d) is a 100 nm sample after cleaning and before measurement. e) 100 nm after measurement.

## 20 nm Pd

The uncycled sample, see figure 4.5a, showed a uniform layer of Pd grains, where the grain size were in the order of some few nm. There were also round rings on the surface of the sample made out of Pd grains. Why these rings appear on the sample is still unknown and more tests should be performed to learn what these formations are. The cycled sample in figure 4.5b showed a large change in grain size compared to the uncycled sample, but it is hard to tell were one grain-boundary start and another ends. A closer look also showed that the ring formation that was seen in the uncycled sample is now gone. Figure 4.5c is a clean sample that



had gone through all the cleaning steps from sonication to CV cleaning, but no real measurements have been performed. This sample showed the same grain size as the sample in figure 4.5a. The sample also showed the same ring formation, but they were slightly less visible.

### 100 nm Pd

The uncycled sample, figure 4.5d, showed uniform layer of Pd grains, where the grain size were of the order of some nm. A closer inspection of the uncycled part of the film, figure 4.5d, showed that it also had the characteristic rings that were clearly visible on the 20 nm film. After the CV was done the cycled area was heavily up scaled, figure 4.5e. The grain size was about 100 nm large, a significant change compared to the uncycled part of the sample. There is however some grains that were much smaller than the rest and this might depend on oxygen corrosion between the CV measurement and the SEM analyze. The larger grains, which implies larger surface area, can also be the reason that the oxide part of the CV in figure 4.4a is slightly larger than its 20 nm counterpart.

## 4.2 Pt thin film measurements

A small number of tests where performed on Pt, evaporated onto a FTO substrate. This was not the main focus but still gave interesting results regarding the optical limit for the UV/Vis measurements.

### 4.2.1 1.5 nm Pt

In figure 4.6a one can clearly see that the tops in the hydrogen absorption region were not as well defined as it would have been on a thicker sample, and the more the sample was cycled the thinner the tops grew. The optical measurements in 4.6b has a lot of noise but can still be seen. The hydrogen and oxygen sorption are clearly visible which shows that measurements on these thin films is possible. The setback is that small films can have problem with drift in the optical signal and that can hinder a correct measurement to be done.

### 4.2.2 0.5 nm Pt

The 0.5 nm Pt sample was a lot harder to extract data from, as the drift from the optical signal was big compared to the signal from the sample itself. This system should be able to acquire some data from, but only if the drift is stabilized in some way.

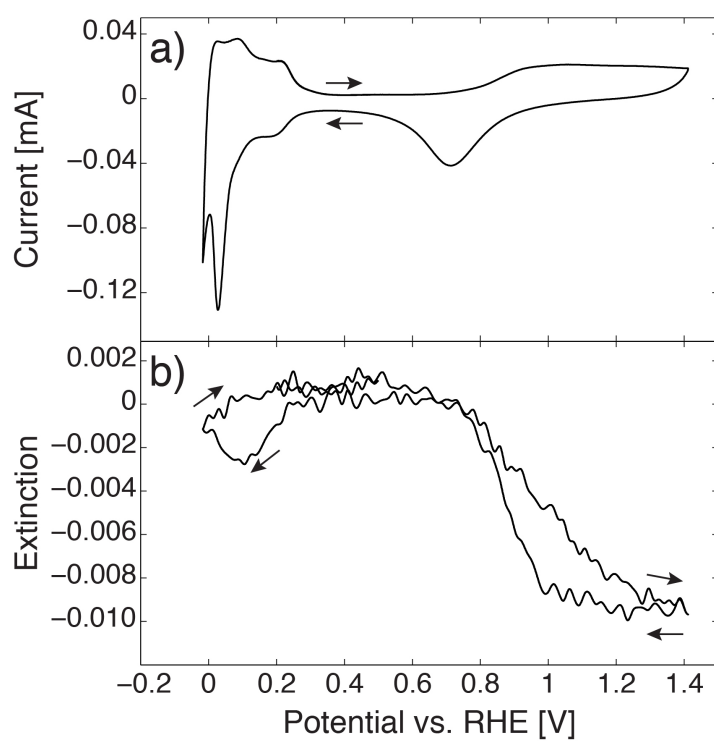


**Figure 4.6:** a) CV for 1.5 nm Pt sample. b) Extinction for a 1.5 nm sample.

# 5

## Conclusion

THE MAIN CONCLUSION is that combining electrochemistry and optical techniques is a powerful tool that can give more understanding of the reactions taking place in, and on, materials used in hydrogen storage research. From this point of view, the results were positive.

With the combination of these techniques it is possible to see when hydride starts to form and when the sample starts to saturate. The CV measurement cannot do this alone due to HER, but with the optic readout it is now possible. With the different optical placements, reflection from bottom, top or transmission, it is possible to see how the different layers (bottom, top and bulk) of the film absorb hydrogen when the electrode is scanned between low and high potentials. Also since reflection measurement can penetrate into a sample it is possible to distinguish between surface and bulk processes by choosing the film thickness so that certain depths are analyzed.

Some of the results presented have some oddities. For example there are still some problems with the flow cell that need to be solved if a broad range of materials shall be used, but the method itself shows good results for the films in 20-100 nm region. For the thinner 0.5 and 1.5 nm Pt films there need to be stable samples before any real conclusion can be made, but even here there are promising results.

Much more research is needed to see the absolute limit of this combination but as far as it has got, it shows great promise for study storage of hydrogen and lifetime of fuel cells. Optimizing the setup can lead to great new discoveries, driving the hydrogen economy even closer to realization.

# 6

## Outlook

### 6.1 Pd outlook

The peak around 0.17 V for the 20 nm films changed depending on the cleaning procedure. A sharper peak was observed from just cycling the whole film from oxide part to the hydride part, and less sharp peak appeared when the "start/stop"-technique was utilized. This "start/stop"-technique is not evaluated so it is unclear if this is the optimal cleaning procedure, and since the tops are moving depending on how you clean your sample more experiments should be performed.

### 6.2 Setup Improvements

During the time of the project it arose a lot of questions and problems around the setup. Some of them could be fixed, but other could not. The biggest problem that occurred was about the limitations of the flow cells ability to handle big currents,  $R_u$  measurements and to some extent measurements on extremely thin films, in this case the 1.5 and 0.5 nm Pt films.

#### 6.2.1 Oxygen formation in the cell

With the current setup there is no possibility to avoid oxygen formation from the CE in the cell when samples that give raise to high currents are used. So for further studies with samples that have high currents, it would be good if there were a cell that has possibilities to exclude this oxygen buildup.

### 6.2.2 Uncompensated Resistance, $R_u$

Another thing that is of importance in the cell is  $R_u$ . In the current form there are two problems, one minor and one major.

The minor problem is that the measurements are done with a grounding cable attach to the spectrometer from the RE, but when doing the simple EIS measurements the ground cable from the RE interfere with the programs ability to extract data. There might not actually be a problem with this, you could detach the cable and doing the simple EIS measurements and then reattach it again. But to be sure that this does not interfere, more test should be done. If the problem persist the spectrometer could be changed to see if another brand gives the same results.

The bigger problem is that the RE is far away from the rest of the electrodes, connected through Tygon<sup>®</sup> tubing. This small tube gives rise to a large resistance. A test done to check the resistance in the tube showed that the tube had a resistance of  $270\Omega/\text{cm}$  (when assuming linear relationship between resistance and length). A more detailed explanation of this test can be seen in appendix A. For samples like Pt this resistance is not so problematic but for a Pd system this could be catastrophic. A cell where the tube between the outlet and the RE is minimized, or even reduced completely is desirable.

### 6.2.3 Drift in optical signal

One particular problem that happened later in the project was the measurement on the thin Pt films. As the film is thin it will also give a low signal back in return. This is problematic due to a constant drift in signal that is observed in the lab. For the 0.5 nm Pt samples the signal to drift ratio was so big that no real conclusions could be done. This system should be able to acquire data from, but only if the drift is stabilized or other equipment, that can neglect the drift, is used.

# Bibliography

- [1] J. Hagberg, Combined electrochemical and optical measurements on Pt and Pd films, Master's thesis, Chalmers University of Technology, Gothenburg, Sweden (2013).
- [2] J. W. Shin, U. Bertocci, G. R. Stafford, In situ stress measurement during hydrogen sorption on ultrathin (111)-textured pd films in alkaline electrolyte 158 (7) (2011) F127–F134.
- [3] The absorption of hydrogen and deuterium in thin palladium electrodes: Part i. acidic solutions, Journal of Electroanalytical Chemistry and Interfacial Electrochemistry 316 (1–2) (1991) 211 – 221.
- [4] Autolab application note (May 2014).  
URL <http://www.autolabj.com/appl.files/appl%20note/App1038.pdf>
- [5] ph calculator - calculates ph of a solution (May 2014).  
URL <http://www.webqc.org/phsolver.php>
- [6] Delamination-supported growth of hydrides in pd thin films studied by electrochemical hydrogenography, Journal of Alloys and Compounds 593 (0) (2014) 87 – 92.
- [7] C. Gabrielli, P. P. Grand, A. Lasia, H. Perrot, Investigation of hydrogen adsorption and absorption in palladium thin films: Ii. cyclic voltammetry 151 (11) (2004) A1937–A1942.
- [8] Electrochemical behaviour of palladium electrode: Oxidation, electrodis-solution and ionic adsorption, Electrochimica Acta 53 (26) (2008) 7583 – 7598.
- [9] Thermodynamics, stress release and hysteresis behavior in highly adhesive pd-h films, International Journal of Hydrogen Energy 36 (6) (2011) 4056 – 4067, 3rd International Workshop in Hydrogen Energy.

## *BIBLIOGRAPHY*

---

- [10] Hydrogen adsorption/absorption on pd/pt(111) multilayers, *Journal of Electroanalytical Chemistry* 621 (1) (2008) 62 – 68.
- [11] Film thickness effects on hydrogen sorption at palladium electrodes, *Journal of Electroanalytical Chemistry and Interfacial Electrochemistry* 106 (0) (1980) 245 – 249.

# A

## $R_u$ -measurements

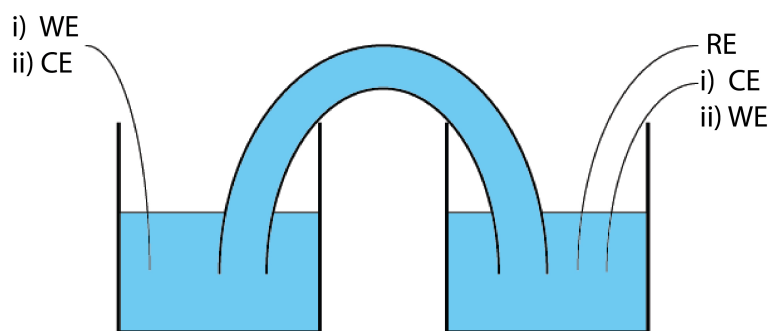


**Figure A.1:**  $R_u$  measurement inspection, comparing different placement of CE and WE (i and ii)

When trying to minimize oxygen formation in the flow cell it was tested to put the CE outside of the cell, beside the RE. There were no bubbles created inside the cell but instead there was a huge increase in  $R_u$ , from around  $16\ \Omega$  up to a total of  $4000\ \Omega$ . To testing this further a simpler setup consisted of two glass beakers and tube between them was used. The length of the tube was changed to be 1.5 times longer compared to the tube for the outlet of the flow cell. Both the WE and the CE were a Pt wire and the RE an  $\text{Hg}/\text{Hg}_2\text{SO}_4$  electrode.

It turned out, that the new  $R_u$ , figure A.1 i), got even higher:  $6000\ \Omega$  (1.5 times higher), when changing the length of the tube from 15 cm to 22.5 cm (1.5 times longer). Swapping the WE and the CE, figure A.1 measure ii), returned the  $R_u$  to around  $16\ \Omega$  again. Assuming a linear relationship between length and  $R_u$  it was calculated that each cm of tubing give approximate  $270\ \Omega$  resistance, a huge contribution considering the  $16\ \Omega$  that was for measure setup ii).



---

Conclusion is then made that the CE cannot be taken outside the flow cell due to high  $R_u$ . It is probable that a tube with a bigger inner diameter can solve the problem, as it allows for a greater flow, but that means that the whole cell needs to be remodelled.